

DMRG in Quantum Chemistry: from concepts to recent applications in (heavy-element) chemistry

PD Dr. Stefan Knecht

Algorithmiq Ltd, Helsinki

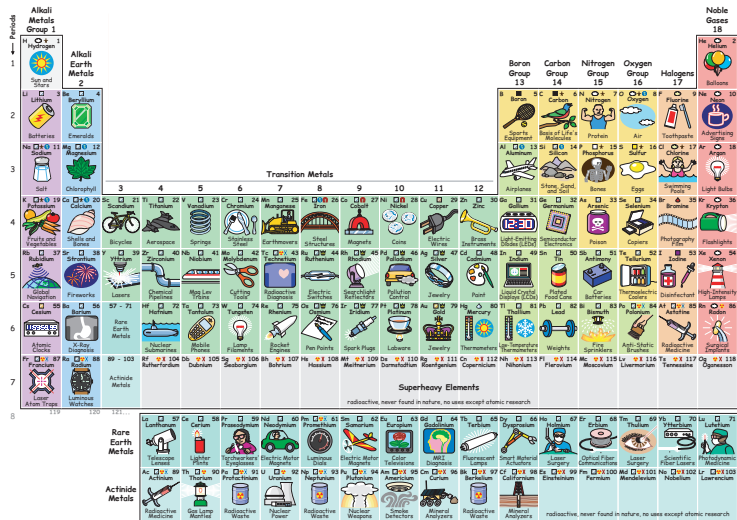
stefan@algorithmiq.fi

Thanks to my long-term collaborators:

Markus Reiher (ETH Zürich), Alberto Baiardi (IBM Zürich), Leon Freitag (QSimulate) and Sebastian Keller (CSC Switzerland)

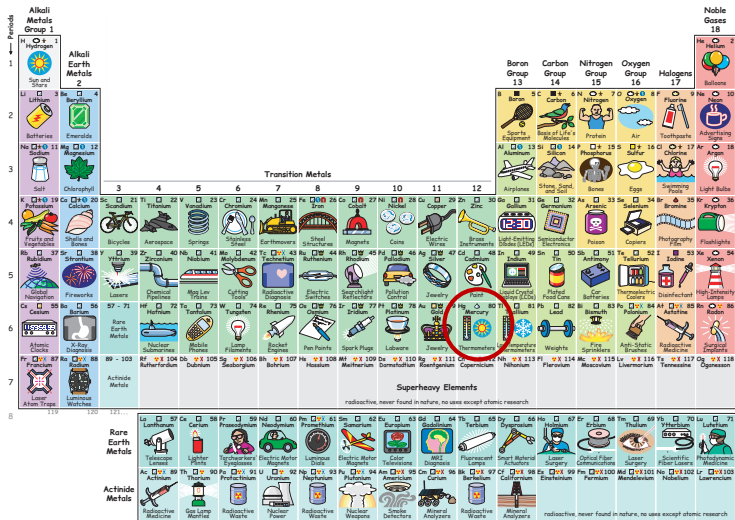
- 1 Motivation
- 2 From CI to MPS: optimizing an MPS with the DMRG algorithm
- 3 Recent developments based on an MPS ansatz

A closer look at the periodic table of elements



© 2005-2016 Keith Enselwood elements.wolfram.com Creative Commons Attribution-ShareAlike 4.0 International License

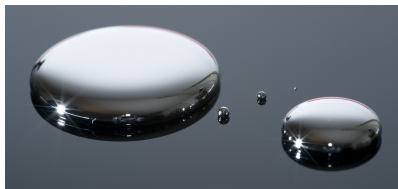
A closer look at the periodic table of elements



© 2005-2016 Keith Enveladen elements.wolark.com Creative Commons Attribution-ShareAlike 4.0 International License

The intriguing case of the liquid state of mercury at room temperature

- Mercury is the only elemental metallic liquid at room temperature
 - Cs: $T_m = 301$ K
 - Ga: $T_m = 303$ K
- Chemical symbol “Hg” → hydragyrum: “liquid silver”
- Why is mercury liquid at room temperature?



Convincing explanations in the literature?

Die erwähnten und nicht erwähnten außergewöhnlichen Quecksilbereigenschaften gehen (...) u. a. darauf zurück, dass (...) durch relativistische Effekte die s -Außenelektronen eine zusätzliche Energieabsenkung (\equiv Orbitalkontraktion), die d -Außenelektronen eine schwache Energieanhebung (\equiv Orbitalexpansion) erfahren.

(Holleman/Wiberg, 103rd edition (2016))

The chemical stability of the $(6s)^2$ family was interpreted as a relativistic effect by Jørgensen (1971, ...). In this sense one could loosely say that “mercury is pseudohelium” due to the relativistic contraction of the $6s$ shell.

*(P. Pyykkö, Adv. Quantum Chem., **11**, 353–409 (1978))*

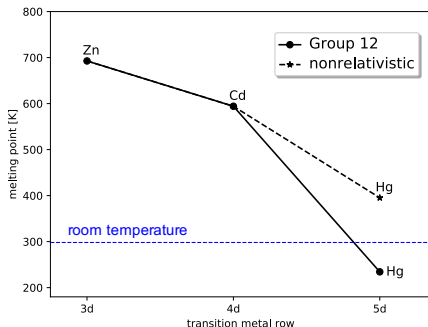
Why is mercury liquid? It is probably because the filled $6s^2$ shell is now more stable. However, explicit proof is still missing.

*(P. Pyykkö, Annu. Rev. Phys. Chem., **63**, 45–64 (2012))*

The intriguing case of the liquid state of mercury at room temperature

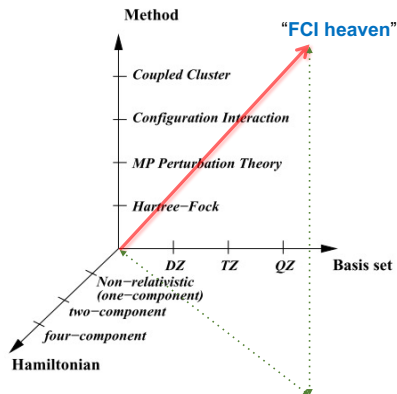
- After ≈ 25 years of intense research **in 2017**:
Ab initio MD simulations of bulk mercury melting unequivocally reveal a **relativistic effect** and – to a smaller extent – electron correlation effects for the melting point T_m :

$$\rightarrow \Delta_{(R-NR)}T_m = -161\text{K}$$



Steenbergen *et al.*, J. Phys. Chem. Lett., **8**, 1407 (2017)

Wave function heaven: systematic improvability



Accurate treatment of electron correlation

- Inclusion of many different electronic configurations
- partially filled, near-degenerate electronic shells
 - multiconfigurational methods
 - (large) active orbital spaces
 - *preferable*: molecular orbital (MO) optimization

Inclusion of relativistic effects

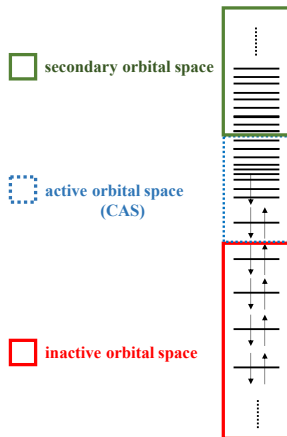
- *preferable*: scalar-relativistic effects
- *possibly*: spin-orbit coupling

Multiconfigurational methods for large active orbital spaces

see also the lectures by Emmanuel Fromager

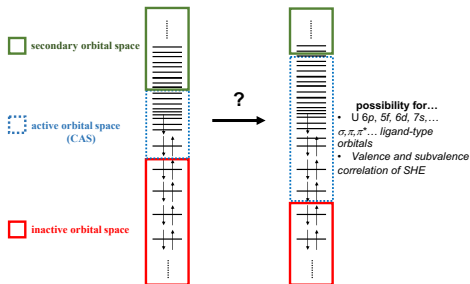
Complete Active Space SCF — CASSCF

Pick an active orbital space (CAS) within which one solves a FCI problem and optimises the MO basis.



The active orbital space problem

- Traditional CASCI hits “exponential” scaling wall at \approx CAS(18,18)



- Requires efficient wave function parametrizations
 - Selected CI (SHCI, CIPSI, ...)
 - QMC (FCIQMC, DMC, ...)
 - Variational 2-RDM
 - **DMRG**
 - ...

Standard CI approach

- CI-type diagonalization for a **preselected** set of many-particle basis states in a given CAS(N, L) (N electrons in L orbitals)

$$|\Psi\rangle = \sum_{k_1, k_2, \dots, k_L} c_{k_1, k_2, \dots, k_L} |k_1\rangle \otimes |k_2\rangle \otimes \dots \otimes |k_L\rangle \quad (1)$$

Density matrix renormalization group

- *Determine* CI coefficients from correlations among orbitals

$$|\Psi\rangle = \sum_{k_1, k_2, \dots, k_L} c_{k_1, k_2, \dots, k_L} |k_1\rangle \otimes |k_2\rangle \otimes \dots \otimes |k_L\rangle \quad (2)$$

- Local space k_l of l -th spatial orbital is of dimension $d = 4$

$$k_l = \{|\uparrow\downarrow\rangle, |\uparrow\rangle, |\downarrow\rangle, |0\rangle\} \quad (3)$$

From CI to MPS: optimizing an MPS with the DMRG algorithm

Optimizing an MPS wave function with the DMRG algorithm

- 1 Optimisation algorithm
- 2 Optimal bipartition
- 3 Parameters that determine DMRG accuracy

Very useful introductory reference:

U. Schollwöck, *The density-matrix renormalization group in the age of matrix product states*, *Annals of Physics*, 326 (2011) 96–192.

Some reviews on about 20 years of DMRG in quantum chemistry

- Ö. Legeza *et al.*, Lect. Notes Phys., 739, 653 (2008)
- G. K.-L. Chan *et al.*, Prog. Theor. Chem. and Phys., 18, 49 (2008)
- D. Zgid and G. K.-L. Chan, Ann. Rep. Comp. Chem., 5, 149, (2009)
- G. K.-L. Chan and S. Sharma, Ann. Rev. Phys. Chem., 62, 465 (2011)
- K. Marti and M. Reiher, Phys. Chem. Chem. Phys., 13, 6750 (2011)
- U. Schollwöck, Ann. Phys., 326, 96 (2011)
- G. K.-L. Chan, WIREs, 2, 907 (2012)
- Y. Kurashige, Mol. Phys., 112, 1485 (2013)
- S. Wouters and D. van Neck, Eur. Phys. J. D, 68, 272 (2014)
- S. Szalay *et al.*, Int. J. Quantum Chem. 115, 1342 (2015)
- T. Yanai *et al.*, Int. J. Quantum Chem., 115, 283 (2015)
- G. K.-L. Chan *et al.*, J. Chem. Phys., 145, 014102 (2016)
- A. Baiardi and M. Reiher, J. Chem. Phys. 152, 040903 (2020)

Intermission: singular value decomposition

- Singular value decomposition (SVD) of a matrix \mathbf{M} ($n_a \times n_b$)

$$\mathbf{M} = \mathbf{U} \mathbf{S} \mathbf{V}^\dagger \quad (4)$$

yields:

- Left-singular matrix \mathbf{U} ($n_a \times \min(n_a, n_b)$) with $\mathbf{U}^\dagger \mathbf{U} = 1$
- Right-singular matrix \mathbf{V} ($\min(n_a, n_b) \times n_b$) with $\mathbf{V}^\dagger \mathbf{V} = 1$
- Diagonal singular value matrix \mathbf{S} ($\min(n_a, n_b) \times \min(n_a, n_b)$) with r nonzero singular values $\rightarrow r$ is the (Schmidt) rank of \mathbf{M}

$$\mathbf{M} = \mathbf{U} \mathbf{S} \mathbf{V}^\dagger \quad \mathbf{M} = \mathbf{U} \mathbf{S} \mathbf{V}^\dagger$$

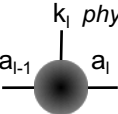
From a CI to an MPS parametrization I

- Successive application of SVD to CI tensor \rightarrow MPS wave function

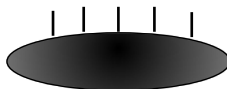

orbital ("site")


matrix


matrix product

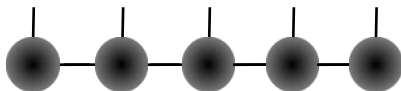

rank-3 tensor

FCI tensor representation



 SVD

MPS representation



From a CI to an MPS parametrization II

- Reshape coefficient tensor c_{k_1, k_2, \dots, k_L} into a $d \times d^{L-1}$ matrix Γ

$$\Gamma_{k_1, (k_2, \dots, k_L)} = c_{k_1, k_2, \dots, k_L} \quad (5)$$

- SVD of $\Gamma_{k_1, (k_2, \dots, k_L)}$ yields

$$\Gamma_{k_1, (k_2, \dots, k_L)} = \sum_{a_1}^{r_1} U_{k_1, a_1} S_{a_1, a_1} (V^\dagger)_{a_1, (k_2, \dots, k_L)} \quad (6)$$

$$\equiv \sum_{a_1}^{r_1} A_{a_1}^{k_1} c_{a_1, (k_2, \dots, k_L)} \quad (7)$$

with

- \mathbf{S} and \mathbf{V}^\dagger multiplied and reshaped into coefficient tensor $c_{a_1, (k_2, \dots, k_L)}$
- $r_1 \leq d$
- collection of d row vectors A^{k_1} with entries $A_{a_1}^{k_1} = U_{k_1, a_1}$

From a CI to an MPS parametrization III

- Reshape coefficient tensor $c_{a_1, (k_2, \dots, k_L)}$ into a $r_1 d \times d^{L-2}$ matrix Γ

$$c_{k_1, k_2, \dots, k_L} = \sum_{a_1}^{r_1} A_{a_1}^{k_1} \Gamma_{(a_1 k_2), (k_3, \dots, k_L)} \quad (8)$$

$$\stackrel{\text{SVD}}{=} \sum_{a_1}^{r_1} \sum_{a_2}^{r_2} A_{a_1}^{k_1} U_{(a_1 k_2), a_2} S_{a_2, a_2} (V^\dagger)_{a_2, (k_3, \dots, k_L)} \quad (9)$$

$$\stackrel{\text{reshape}}{\equiv} \sum_{a_1}^{r_1} \sum_{a_2}^{r_2} A_{a_1}^{k_1} A_{a_1, a_2}^{k_2} \Gamma_{(a_2 k_3), (k_4, \dots, k_L)} \quad (10)$$

with

- $r_2 \leq r_1 d \leq d^2$
- collection of d matrices A^{k_2} with entries $A_{a_1, a_2}^{k_2} = U_{(a_1 k_2), a_2}$

From a CI to an MPS parametrization IV

- Continue with SVDs until last site which then gives

$$c_{k_1, k_2, \dots, k_L} = \sum_{a_1, a_2, \dots, a_{L-1}} A_{1, a_1}^{k_1} A_{a_1, a_2}^{k_2} \dots A_{a_{L-2}, a_{L-1}}^{k_{L-1}} A_{a_{L-1}, 1}^{k_L} \quad (11)$$

$$\equiv A^{k_1} A^{k_2} \dots A^{k_{L-1}} A^{k_L} \quad (12)$$

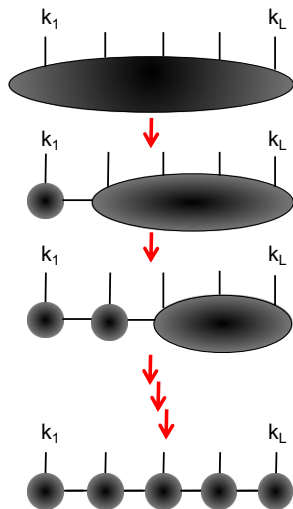
with

- interpretation of sums as matrix-matrix multiplications
 - first and last “matrices” are row- and column vectors!
- CI wave function rewritten as MPS wave function:

$$|\Psi\rangle = \sum_{\mathbf{k}} c_{\mathbf{k}} |\mathbf{k}\rangle = \sum_{k_1, k_2, \dots, k_L} A^{k_1} A^{k_2} \dots A^{k_{L-1}} A^{k_L} |\mathbf{k}\rangle \quad (13)$$

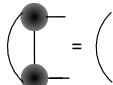
From a CI to an MPS parametrization V

... *schematically*



Properties of the MPS I

- Matrix dimensions grow exponentially up to $\dim(d^{L/2-1} \times d^{L/2})$
if no truncation occurs, i.e., all singular values are kept
→ **Optimal truncation scheme (in a least-square sense) required!**
- From $U^\dagger U = I$ follows that all matrices $\{A^{k_l}\}$ are **left-normalized**

$$\sum_{k_l} A^{k_l \dagger} A^{k_l} = I \quad (14)$$


- MPS built from left-normalized matrices is called **left-canonical**
- For any lattice bipartition at site l , the states on sites $1, \dots, l$

$$|a_l\rangle_{\mathcal{L}} = \sum_{k_1, k_2, \dots, k_l} \left(A^{k_1} \dots A^{k_l} \right)_{1, a_l} |k_1, \dots, k_l\rangle \quad (15)$$

span a left subsystem \mathcal{L} and form an orthonormal basis

Properties of the MPS II

- Starting SVD on coefficient tensor in Eq. (5) from right-hand side

$$\Gamma_{(k_1, k_2, \dots, k_{L-1}), k_L} = c_{k_1, k_2, \dots, k_L} \quad (16)$$

yields **right-normalized** matrices $\{B^{k_l}\}$ (as $V^\dagger V = I$), e.g.,

$$\sum_{k_l} B^{k_l} B^{k_l \dagger} = I \quad (17) \quad \left(\begin{array}{c} \bullet \\ | \\ \bullet \end{array} \right) =$$

- MPS built from right-normalized matrices is called **right-canonical**
- For any lattice bipartition at site $l + 1$, states on $l + 1, \dots, L$

$$|a_l\rangle_{\mathcal{R}} = \sum_{k_{l+1}, k_{l+2}, \dots, k_L} \left(B^{k_{l+1}} \dots B^{k_L} \right)_{a_l, 1} |k_{l+1}, \dots, k_L\rangle \quad (18)$$

span a right subsystem \mathcal{R} and form an orthonormal basis

Gauge freedom and mixed-canonical form

- MPS representations are not unique \leftrightarrow existence of a gauge degree of freedom
- Consider two adjacent matrices M^{k_l} and $M^{k_{l+1}}$ of shared column/row dimension D and a square invertible matrix X ($D \times D$)
- Invariance of MPS immediately follows from

$$M^{k_l} \rightarrow M^{k_l} X; \quad M^{k_{l+1}} \rightarrow X^{-1} M^{k_{l+1}} \quad (19)$$

since

$$M^{k_l} \underbrace{X X^{-1}}_{=I} M^{k_{l+1}} = M^{k_l} \cdot M^{k_{l+1}} \quad (20)$$

- Gauge freedom allows to write an MPS in **mixed canonical** form at sites $\{l, l + 1\}$

$$|\Psi\rangle = \sum_{\mathbf{k}} A^{k_1} \dots A^{k_{l-1}} M^{k_l k_{l+1}} B^{k_{l+2}} \dots B^{k_L} |\mathbf{k}\rangle \quad (21)$$

by starting from a general MPS wave function

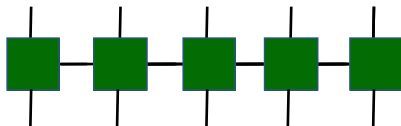
$$|\Psi\rangle = \sum_{\mathbf{k}} M^{k_1} M^{k_2} \dots M^{k_L} |\mathbf{k}\rangle \quad (22)$$

and the two-site MPS tensor in Eq. (21) reading as

$$M^{k_l k_{l+1}} \equiv M_{a_{l-1}, a_{l+1}}^{k_l k_{l+1}} = \sum_{a_l} M_{a_{l-1}, a_l}^{k_l} M_{a_l, a_{l+1}}^{k_{l+1}} \quad (23)$$

Matrix product operators I

- MPS concept applied to operators \rightarrow matrix product operators (MPOs)



- N -electron operator \widehat{W} in MPO form

$$\widehat{W} = \sum_{\mathbf{k}\mathbf{k}'} \sum_{b_1, \dots, b_{L-1}} W_{1,b_1}^{k_1 k'_1} W_{b_1, b_2}^{k_2 k'_2} \dots W_{b_{L-1}, 1}^{k_L k'_L} |\mathbf{k}\rangle \langle \mathbf{k}'| \quad (24)$$

$$= \sum_{\mathbf{k}\mathbf{k}'} W^{k_1 k'_1} W^{k_2 k'_2} \dots W^{k_L k'_L} |\mathbf{k}\rangle \langle \mathbf{k}'| \quad (25)$$

$$\equiv \sum_{\mathbf{k}\mathbf{k}'} w_{\mathbf{k}\mathbf{k}'} |\mathbf{k}\rangle \langle \mathbf{k}'| \quad (26)$$

Matrix product operators II

- For efficiency, rearrange summations in Eq. (24) such that the contraction proceeds first over the local site indices $k_l k'_l$

$$W_{b_{l-1}, b_l}^l = \sum_{k_l k'_l} W_{b_{l-1}, b_l}^{k_l k'_l} |k_l\rangle \langle k'_l| . \quad (27)$$

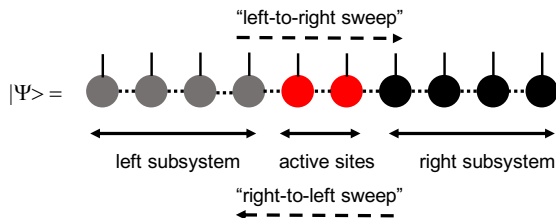
- By means of Eq. (27) we can write Eq. (24) as

$$\widehat{W} = \sum_{b_1, \dots, b_{L-1}} W_{1, b_1}^1 \cdots W_{b_{l-1}, b_l}^l \cdots W_{b_{L-1}, 1}^L . \quad (28)$$

- **Note:** the entries of $\{W_{b_{l-1}, b_l}^l\}$ matrices comprise the elementary, *local* operators acting on the l -th orbital, e.g.,

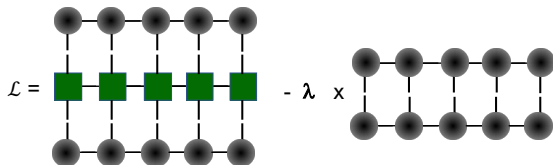
$$\tilde{a}_{\uparrow l}^\dagger = |\uparrow\downarrow\rangle \langle\downarrow| + |\uparrow\rangle \langle 0| \quad (29)$$

Variational MPS optimization I



- Goal: find optimal approximation $|\tilde{\Psi}\rangle$ to $|\Psi\rangle$ (in a least-square sense)
- Prerequisite: initialize suitable (valid) trial MPS wave function $|\tilde{\Psi}\rangle$
 - choices for warm-up guess: random guess, encode HF determinant, CI-DEAS by Ö. Legeza, ...
 - assume normalization, i.e., $\langle\Psi|\Psi\rangle = 1$

Variational MPS optimization II



- *Ansatz* for variational MPS optimization: extremize the Lagrangian

$$\mathcal{L} = \langle \Psi | \hat{H} | \Psi \rangle - \lambda \langle \Psi | \Psi \rangle \quad (30)$$

with the two-site $\{M^{k_l k_{l+1}}\}$ matrices as optimization parameters

- Optimize at each step of a “sweep” entries of site matrices of **two orbitals** (“two-site DMRG”) while keeping all the others fixed
- Sweep through all sites multiple times until energy converges

Variational MPS optimization III

- At sites $\{l, l + 1\}$, take derivative in Eq. (30) with respect to complex conjugate of $M^{k_l, k_{l+1}}$

$$\frac{\partial}{\partial M^{k_l, k_{l+1}*}} (\langle \Psi | \hat{H} | \Psi \rangle - \lambda \langle \Psi | \Psi \rangle) = 0 \quad (31)$$

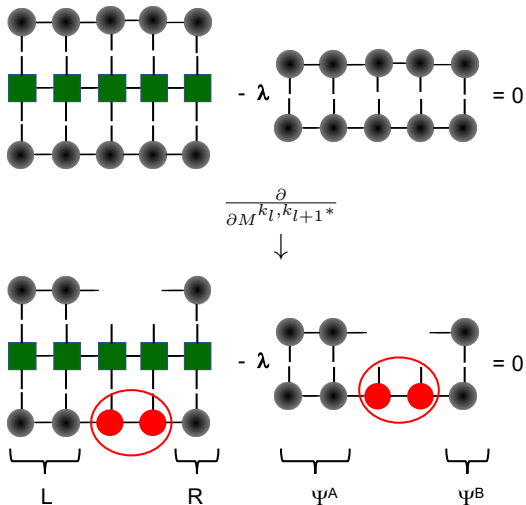
which then yields

$$\sum_{\substack{a'_{l-1} a'_l \\ b_{l-1} b_{l+1}}} \sum_{k'_l k'_{l+1}} L_{a_{l-1}, a'_{l-1}}^{b_{l-1}} W_{b_{l-1}, b_{l+1}}^{k_l k_{l+1}, k'_l k'_{l+1}} R_{a'_{l+1}, a_{l+1}}^{b_{l+1}} M_{a'_{l-1}, a'_{l+1}}^{k'_l k'_{l+1}} = \lambda \sum_{a'_{l-1} a'_l} \Psi_{a'_{l-1}, a_{l-1}}^A \times M_{a'_{l-1}, a'_{l+1}}^{k'_l k'_{l+1}} \times \Psi_{a'_{l+1}, a_{l+1}}^B \quad (32)$$

- L and R are the so-called *left* and *right boundaries* obtained by contracting the MPO with the bra and ket MPS starting from left (right) up to sites $l - 1$ ($l + 1$)

Variational MPS optimization IV

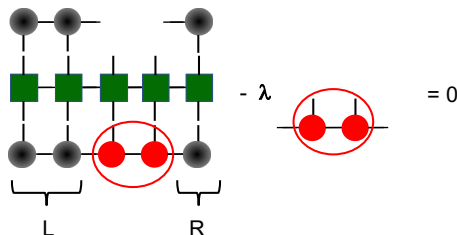
- Schematically



Variational MPS optimization V

- NB: Eq. (32) defines a *generalized eigenvalue problem* which can be simplified to a *standard eigenvalue problem* (Eq. (33)) if the MPS is a canonical MPS!
- The latter requires the initial MPS to be right-normalized!
- Hence, assuming correct normalization Eq. (32) simplifies to

$$\sum_{\substack{a'_{l-1} a'_l \\ b_{l-1} b_{l+1}}} \sum_{k'_l k'_{l+1}} L_{a_{l-1}, a'_{l-1}}^{b_{l-1}} W_{b_{l-1}, b_{l+1}}^{k_l k_{l+1}, k'_l k'_{l+1}} R_{a'_{l+1}, a_{l+1}}^{b_{l+1}} M_{a'_{l-1}, a'_{l+1}}^{k'_l k'_{l+1}} = \lambda M_{a'_{l-1}, a'_{l+1}}^{k'_l k'_{l+1}} \quad (33)$$



Variational MPS optimization VI

- Recast Eq. (33) into a matrix eigenvalue equation

$$\mathcal{H}v - \lambda v = 0, \quad (34)$$

- by defining a local Hamiltonian matrix \mathcal{H} at sites $\{l, l + 1\}$

$$H_{(k_l k_{l+1} a_{l-1} a_{l+1}), (k'_l k'_{l+1} a'_{l-1} a'_{l+1})} = \sum_{b_{l-1}, b_{l+1}} L_{a_{l-1}, a'_{l-1}}^{b_{l-1}} W_{b_{l-1}, b_{l+1}}^{k_l k_{l+1}, k'_l k'_{l+1}} R_{a'_{l+1}, a_{l+1}}^{b_{l+1}}$$

- and a vector v

$$v_{k'_l k'_{l+1} a'_{l-1} a'_{l+1}} = M_{a'_{l-1}, a'_{l+1}}^{k'_l k'_{l+1}}.$$

- Solve Eq. (34) by an iterative eigensolver

→ eigenvalue λ^0 and corresponding eigenvector $v_{k'_l k'_{l+1} a'_{l-1} a'_{l+1}}^0$

Variational MPS optimization VII

- Reshape $v_{k'_l k'_{l+1} a'_{l-1} a'_{l+1}}^0$ back to $M_{a'_{l-1}, a'_{l+1}}^{k'_l k'_{l+1}}$
- $M_{a'_{l-1}, a'_{l+1}}^{k'_l k'_{l+1}}$ is subsequently subject to a left- or right-normalization
$$M_{a'_{l-1}, a'_{l+1}}^{k'_l k'_{l+1}} = M_{(k'_l, a'_{l-1})(k'_{l+1}, a'_{l+1})} = U_{(k'_l, a'_{l-1})s_l} S_{s_l s_l} V_{s_l(a'_{l+1}, k'_{l+1})} \quad (35)$$
- By **discarding** the $3m$ smallest singular values in $S_{s_l s_l}$ to obtain $S_{a'_l a'_l}$ we achieve the **desired reduction in bond dimensionality!**
- The maximum (fixed) number m of retained singular values is usually called **number of renormalized block states**

Variational MPS optimization VIII

- Discarding the $3m$ smallest singular values corresponds to discarding the last $3m$ columns (rows) of U (V) such that for the two site matrices $M_{a'_{l-1}, a'_l}^{k'_l}$ and $M_{a'_l, a'_{l+1}}^{k'_{l+1}}$ we obtain

$$M_{a'_{l-1}, a'_l}^{k'_l} = U_{(k'_l, a'_{l-1})a'_l} \quad (36)$$

$$M_{a'_l, a'_{l+1}}^{k'_{l+1}} = \frac{1}{1 - \sum_{s_l=m+1}^{4m} S_{s_l s_l}} S_{a'_l a'_l} V_{a'_l (a'_{l+1}, k'_{l+1})} \quad (37)$$

- Energy calculated as a function of the truncation error ϵ

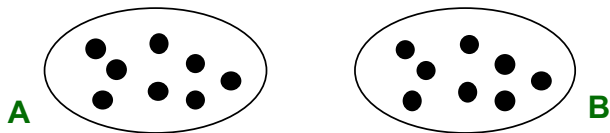
$$\epsilon = \sum_{s_l=m+1}^{4m} S_{s_l s_l} = \|\Psi_{16m^2} - \Psi_{4m^2}\| \quad (38)$$

can be employed to obtain an error estimate through extrapolation

Variational MPS optimization IX

- Moving from sites $\{l, l + 1\}$ to sites $\{l + 1, l + 2\}$ completes the local optimization step
- **BUT:** Is the chosen approximation optimal in a least-square sense as we set out to do so?

Optimal bipartition in a least square sense I

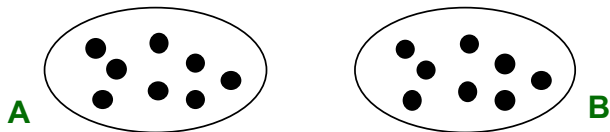


- Given: many-body state $|\Psi\rangle$ of composite system **AB**

$$|\Psi\rangle = \sum_{ij} C_{ij} |i\rangle_A \otimes |j\rangle_B \quad (39)$$

- $\{|i\rangle_A\}$ ($\{|j\rangle_B\}$) are orthonormal bases of **A** (**B**) with dimension N_A (N_B)

Optimal bipartition in a least square sense II



- SVD of $|\Psi\rangle$ yields

$$|\Psi\rangle = \sum_{ij} \sum_{a=1}^{\min(N_A, N_B)} U_{ia} S_{aa} V_{ja}^* |i\rangle_A |j\rangle_B \quad (40)$$

$$= \sum_{a=1}^{\min(N_A, N_B)} \left(\sum_i U_{ia} |i\rangle_A \right) s_a \left(\sum_j V_{ja}^* |j\rangle_B \right) \quad (41)$$

$$= \sum_{a=1}^{\min(N_A, N_B)} s_a |a\rangle_A |a\rangle_B \quad (42)$$

Optimal bipartition in a least square sense III

- Restricting the sum in Eq.(42) to some value $r \leq \min(N_A, N_B)$ yields the *Schmidt decomposition*

$$|\Psi\rangle = \sum_{a=1}^r s_a |a\rangle_A |a\rangle_B \quad (43)$$

where $r = 1$ corresponds to (classical) product states and $r > 1$ to entangled (quantum) states

- For orthonormal states in **A** and **B**, the two-norm $\|\Psi\|_2^2$ is identical to the Frobenius norm of the matrix $\{C_{ij}\}$, $\|\mathbf{C}\|_F^2$

$$\|\Psi\|_2^2 = \|\mathbf{C}\|_F^2 = \sum_{a=1}^{\min(N_A, N_B)} s_a^2 \quad (44)$$

Optimal bipartition in a least square sense IV

- Hence, an optimal approximation $|\tilde{\Psi}\rangle$ to $|\Psi\rangle$ with respect to the 2-norm immediately follows from optimal approximation of \mathbf{C} by $\tilde{\mathbf{C}}$ in the Frobenius norm, with $\tilde{\mathbf{C}}$ being a matrix of rank $r' \leq r$

$$|\tilde{\Psi}\rangle = \sum_{a=1}^{r'} s_a |a\rangle_A |a\rangle_B \quad (45)$$

- BUT** how does this relate to the truncation (dimensionality reduction) in the variational MPS optimization?

Optimal bipartition in a least square sense V

- Last line in Eq. (42) can be realized for site l by an MPS in mixed-canonical form (cf. Eq. (21))

$$|\Psi\rangle = \sum_{\mathbf{k}} A_{1,a_1}^{k_1} \cdots A_{a_{l-1},a_l}^{k_l} S_{a_l,a_l} B_{a_l,a_{l+1}}^{k_{l+1}} \cdots B_{a_{L-1},1}^{k_L} |\mathbf{k}\rangle \quad (46)$$

$$= \sum_{a_l} \left(\sum_{\substack{k_1, \dots, k_l \\ a_1, \dots, a_{l-1}}} A_{1,a_1}^{k_1} \cdots A_{a_{l-1},a_l}^{k_l} |k_1, \dots, k_l\rangle \right) \cdot S_{a_l,a_l} \cdot \left(\sum_{\substack{k_{l+1}, \dots, k_L \\ a_{l+1}, \dots, a_{L-1}}} B_{a_l,a_{l+1}}^{k_{l+1}} \cdots B_{a_{L-1},1}^{k_L} |k_{l+1}, \dots, k_L\rangle \right) \quad (47)$$

$$= \sum_{a_l} S_{a_l,a_l} |a_l\rangle_{\mathcal{L}} |a_l\rangle_{\mathcal{R}} \quad (48)$$

- Comparison of Eqs. (48) and (43) immediately reveals that *an optimal bipartition in a least square sense* can be obtained for $|\tilde{\Psi}\rangle$ from an SVD retaining the lowest r ($\equiv m$ as usually referred to in DMRG terminology) values with $r < \dim(|\Psi\rangle)$

$$|\tilde{\Psi}\rangle = \sum_{a_l=1}^r S_{a_l a_l} |a_l\rangle_{\mathcal{L}} |a_l\rangle_{\mathcal{R}} \quad (49)$$

Scaling of variational MPS optimization

- Scaling is dominated by the cost of contracting the operator with the MPS on one site and is proportional to the number of non-zero elements in the MPO matrices $\{\widehat{W}\}$
 - in a naïve MPO ansatz this step scales as $\mathcal{O}(L^5)$
 - in an optimized code scaling reduces to $\mathcal{O}(L^4)$

[Keller, Dolfi, Troyer, Reiher, J. Chem. Phys., 143, 244118 \(2015\)](#)

- Further reduction through symmetry: $U(1)$ and $SU(2)$

[Keller and Reiher, J. Chem. Phys., 144, 134101 \(2016\)](#)

- SVD scales as $\mathcal{O}(m^3)$ (but there are L of them in a sweep)
- Taking into account all operations a sweep scales $\approx \mathcal{O}(L^4 m^3)$

[Wouters and van Neck, Eur. Phys. J. D, 68, 272 \(2014\)](#)

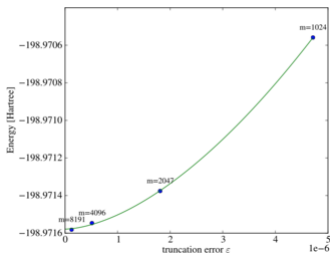
Extrapolation

- Extrapolate E based on truncation error ϵ for different values of m

$$\ln \left(\frac{E_{\text{DMRG}} - E_{\text{FCI}}}{E_{\text{FCI}}} \right) = a \ln \epsilon + b \quad (50)$$

Ö. Legeza, *et al.*, Phys. Rev. B, 67, 124114 (2003)

- Example: ground-state calculation for F_2 molecule



S. Keller, M. Reiher, *Chimia*, 68, 200 (2014)

DMRG

- Variational
- Size consistent
- (approximate) FCI for a CAS
- Polynomial scaling ($\approx L^4 m^3$)
- MPS wave function
- For large m invariant wrt orbital rotations

CASCI

- Variational
- Size consistent
- FCI for a CAS
- Factorial scaling
- Linearly parametrized wave function
- Invariant wrt orbital rotations

Determining factors of DMRG convergence

- Size L of the CAS
- Type of molecular orbitals (HF, NO's, localized orbitals, . . .)
- Guess of states in the right subsystem in the first sweep (for example CI-DEAS by Ö. Legeza or random guess)
- Ordering of orbitals (exploit entanglement measures)

Stein, Reiher, J. Chem. Theory Comput., 12, 1760 (2016)

- Number of renormalized block states m

NB: One should never calculate results for just a single m , but increase it in various runs until results converge!

Publicly available quantum-chemistry centric DMRG packages

Disclaimer: list might be incomplete

- CheMPS2: <https://github.com/SebWouters/CheMPS2>
(discontinued but still a versatile code)
- QCMAquis: <https://github.com/qcscine/qcmaquis>
(actively developed; contains a number of unique features)
- Block2: <https://github.com/block-hczhai/block2-preview>
(most versatile and actively developed DMRG code; probably the best on the “market”)

Intermission: Assessing electron correlation effects

- Exploit the “regularization“ effect in a hybrid range-separated **short-range DFT/long-range MPS** ansatz to distinguish strong from dynamical electron correlation effects
- Based on the decomposition of two-electron repulsion into long- and short-range contributions,

$$1/r_{12} = w_{ee}^{\text{lr},\mu}(r_{12}) + w_{ee}^{\text{sr},\mu}(r_{12}) , \quad (51)$$

$$w_{ee}^{\text{lr},\mu}(r_{12}) = \text{erf}(\mu r_{12})/r_{12} , \quad (52)$$

→ range separation parameter $\mu \in [0, +\infty[$

Based on ideas originally proposed by A. Savin

- CAS-CI-like energy expression becomes

$$E_{\text{MPS-CI}}^{\text{srDFT}} = E_{\text{I}}^{\text{lr}} + E_{\text{A}}^{\text{lr}} + E_{\text{H}}^{\text{sr}}[n] + E_{\text{xc}}^{\text{sr}}[n] \quad (53)$$

Assessing electron correlation effects II

- Use measures obtained from quantum information theory to quantify orbital correlations
- Single-orbital von Neumann entropy $s_i(1)$

$$s_i(1) = - \sum_{\alpha=1}^4 n_{\alpha,i} \ln(n_{\alpha,i}), \quad (54)$$

where $n_{\alpha,i}$ are the eigenvalues of the **one-orbital** RDM

- Mutual information I_{ij} between orbitals i and j is defined in terms of $s_i(1)$ and $s_{ij}(2)$

$$I_{ij} = (s_i(1) + s_j(1) - s_{ij}(2)) (1 - \delta_{ij}) \quad (55)$$

Ö. Legeza and J. Solyom, Phys. Rev. B 68, 195116 (2003)

Ö. Legeza and J. Solyom, Phys. Rev. B 70, 205118 (2004)

Assessing electron correlation effects III

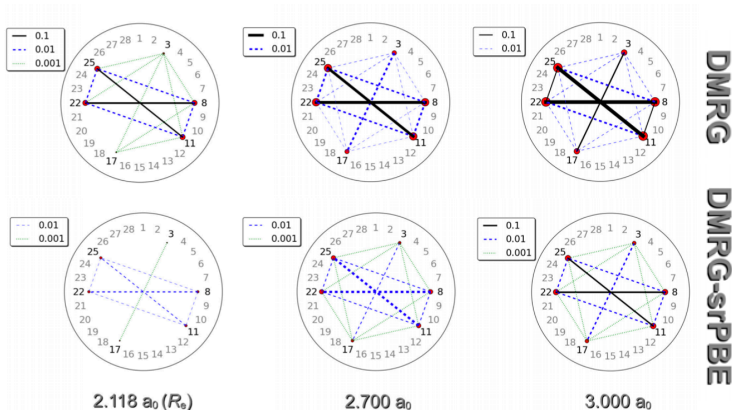
One-orbital RDM contains elements of the 1- and 2-RDM!

$$\rho_i(1) = \begin{pmatrix} 1 - \gamma_i^i - \gamma_{\bar{i}}^{\bar{i}} + \Gamma_{i\bar{i}}^{i\bar{i}} & 0 & 0 & 0 \\ 0 & \gamma_i^i - \Gamma_{i\bar{i}}^{i\bar{i}} & 0 & 0 \\ 0 & 0 & \gamma_{\bar{i}}^{\bar{i}} - \Gamma_{i\bar{i}}^{i\bar{i}} & 0 \\ 0 & 0 & 0 & \Gamma_{i\bar{i}}^{i\bar{i}} \end{pmatrix} \quad (56)$$

Two-orbital RDM contains elements of the 1-, 2-, 3- and 4-RDM!

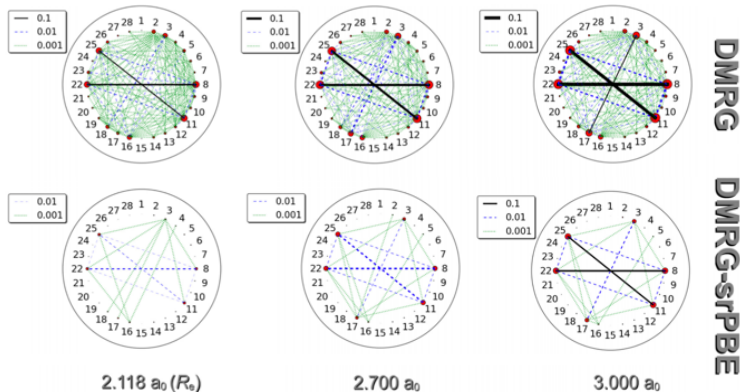
Boguslawski and Tecmer, I. J. Quant. Chem., 115, 1289 (2015)

Stretching N₂...



Hedegaard, Knecht, Kielberg, Jensen, Reiher, J. Chem. Phys., 142, 224108 (2015)

Stretching N2...



Hedegaard, Knecht, Kielberg, Jensen, Reiher, J. Chem. Phys., 142, 224108 (2015)

Accurate treatment of electron correlation

- Inclusion of many different electronic configurations
- partially filled, near-degenerate electronic shells
 - multiconfigurational methods
 - (large) active orbital spaces
 - *preferable*: MO optimization

Inclusion of relativistic effects

- *preferable*: scalar-relativistic effects
- *possibly*: spin-orbit coupling

What are “relativistic effects”?

What is relativity?

The principle of relativity requires that the equations describing the laws of physics have the same form in all inertial frames, i.e. for different observers

Galilean principle of relativity

- Newton's law of motion ($\vec{F} = m \cdot \vec{a}$) has the same form in all inertial frames of reference
- Speed of light c depends on the motion of the observer

Einsteinian principle of relativity

- Maxwell's equations of motion for electromagnetic waves have the same form in all inertial frames of reference
- Speed of light c is the same in all inertial frames of reference

Identifying the true principle of relativity

- Hard experimental evidence that all observers in all inertial frames always measure the same speed of light

$$c' = c = \text{const.} \quad \forall (\text{inertial frames})'$$

Michelson–Morley interferometer experiment (1887)

- Galilean principle of relativity is to be abandoned
Newton's laws cannot be fundamental laws of nature!
- Relativity principle of Einstein is correct
Maxwell's equations of motion are fundamental laws of nature!

“Picking” the proper quantum mechanics

Describing the molecular world requires a quantum mechanical theory!

Schrödinger quantum mechanics

- Follows from the *correspondence principle* applied to Newton's law of motion



Dirac quantum mechanics

- Fully consistent with Einsteinian principle of relativity
- Schrödinger quantum mechanics is obtained in the limit $c \rightarrow \infty$

What are “relativistic effects”?

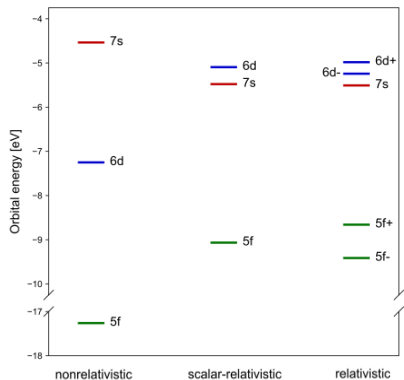
What are “relativistic effects”?

“Relativistic effects” are a hypothetical construct denoting the difference between a relativistic (Dirac QM \leftrightarrow Einsteinian POR) and a nonrelativistic (Schrödinger QM \leftrightarrow Galilean POR) description of matter

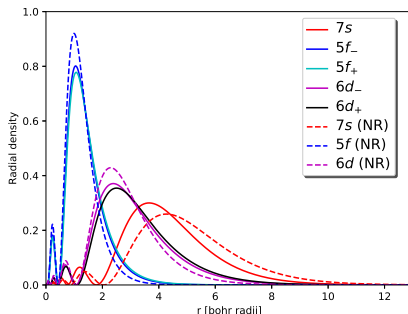
- Two kinds of “relativistic effects” are commonly distinguished:
 - **kinematic** (or **scalar-relativistic**) **effects**
 - **spin-orbit (SO) coupling**
- A different distinction useful for chemistry:
 - **direct relativistic effects**: *relativistic contraction* of (inner) s and p shells and SO coupling
 - **indirect relativistic effects**: *relativistic expansion* of the outer d and f shells (screening effects)

Relativistic effects in the uranium atom

- **Direct effect:** energetic stabilization of the $7s$ shell
- **Indirect effect:** energetic destabilization of the $5f/6d$ shells



- **Direct effect:** radial contraction of the $7s$ shell
- **Indirect effect:** radial expansion of the $5f/6d$ shells



One-step approaches

“j-j coupling”

- *Ab initio* inclusion of SO coupling & scalar-relativistic effects
- Use Dirac Hamiltonian in a **four-component**
or
two-component (“electrons-only”) form

Two-step approaches

“L-S coupling”

- *A posteriori* inclusion of SO coupling by state interaction

$$\mathbf{Hc} = E\mathbf{Sc}$$

- Express \mathbf{H} in the basis of eigenfunctions of $\hat{\mathcal{H}}^{(0)}$
- Use Hamiltonian of form

$$\hat{\mathcal{H}} = \hat{\mathcal{H}}^{(0)} + \hat{\mathcal{H}}^{SO}$$

Recent MPS-based applications in (heavy-element) chemistry

Many beautiful and original works of DMRG in QC by pioneers in the field

- Ö. Legeza
- Garnet Chan
- Takeshi Yanai
- Marcel Nooijen
- Yuki Kurashige
- Dominika Szgid
- Sandeep Sharma
- Dimitry van Neck
- Sebastian Wouters
- . . . many other whom I might have forgotten to mention here

A biased view on our work within (relativistic) quantum chemistry with DMRG

- Excited states
- Magnetic properties
- Shell structures of (super-)heavy elements
- Electronic structure in strong magnetic fields

Electronic structure theory for f -elements



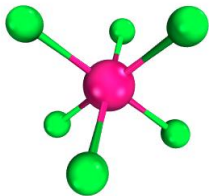
Ground- and excited-state properties of [U]-complexes

Uranium hexachlorides (UCl_6) $^{q-}$ ($q = 1, 2$)

Knecht, unpublished

- Relativistic 4c-DMRG-SCF calculations ($m = 1024$)
- State-averaged optimization
 - (UCl_6) $^{1-}$: 14 roots
 - (UCl_6) $^{2-}$: 17 roots
- Basis sets
 - U: *uncontracted* ANO-RCC
 - Cl: ANO-RCC-TZVP
- Customized fitting basis sets
- Excitation energies in eV

- octahedral f^1 and f^2 complexes



Uranium hexachlorides (UCl_6) $^{q-}$ ($q = 1, 2$)

Knecht, unpublished

- Ground- and excited-state properties of (UCl_6) $^{1-}$

state	aU _{3/2u}	aE _{5/2u}	bU _{3/2u}	aE _{1/2u}	<i>g</i> -factor
CAS(7,20)	0.41	0.91	1.31	1.48	-1.15
CAS(19,32) [†]	0.46	0.85	1.32	1.48	-
CAS(19,32) [‡]	0.46	0.82	1.30	1.46	-
experiment ^a	0.47	0.84	1.26	1.43	-1.1
CAS-SOC ^b	-	0.89	1.34	1.53	-1.05
SO-CASPT2 ^c	0.47	0.91	1.39	1.54	-1.06
CAS/CCSD(T)/SO ^d	0.39	0.73	1.13	1.30	-

[†] Dirac-Coulomb; [‡] Dirac-Coulomb-Breit

^a Selb *et al.*, Inorg. Chem., 7, 976 (1968); ^b Ganyushin and Neese, J. Chem. Phys., 138, 104113 (2013)

^c Notter and Bolvin, J. Chem. Phys., 130, 184310 (2009); ^d Su *et al.*, J. Chem. Phys., 142, 134308 (2015)

Uranium hexachlorides (UCl_6) $^{q-}$ ($q = 1, 2$)

Knecht, unpublished

- Ground- and excited-state properties of (UCl_6) $^{2-}$

state	aT _{1g}	aE _g	aT _{2g}	bE _g	bT _{2g}	bT _{1g}
CAS(2,14) [†]	0.10	0.15	0.27	0.77	0.77	0.78
CAS(2,14) [‡]	0.10	0.15	0.27	0.76	0.76	0.76
CAS(20,32)	0.10	0.15	0.26	0.68	0.72	0.80
experiment ^a	0.11	0.16	0.28	0.63	0.61	0.79
SO-CASPT2 ^b	0.09	0.14	0.24	0.66	0.67	0.66

[†] Dirac-Coulomb; [‡] Dirac-Coulomb-Breit

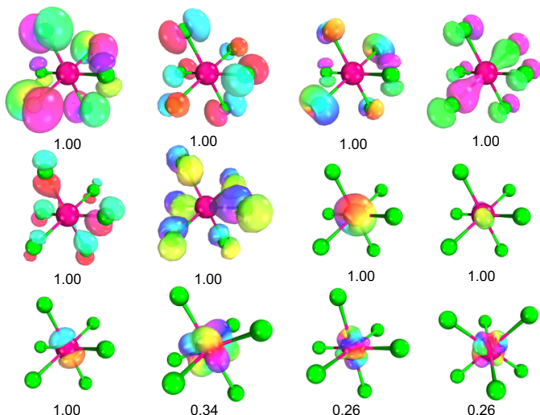
^a Flint *et al.*, *Mol. Phys.*, 61, 389 (1987); ^b Su *et al.*, *J. Chem. Phys.*, 142, 134308 (2015)

- g-factor in the A_{1g} ground state: g_{||}=0.57 (0.58), g_⊥=1.92 (1.91)

Uranium hexachlorides (UCl_6) $^{q-}$ ($q = 1, 2$)

Knecht, unpublished

- Valence spinors (only one Kramers-partner shown) of (UCl_6) $^{2-}$



hue of the colors represents the spinor's phase

Al-Saadon *et al.*, *J. Phys. Chem. A*, 123, 3223 (2019)

Magnetic properties of a [Dy]-complex

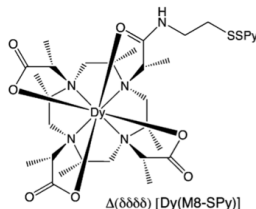
Battaglia, Keller, Knecht, J. Chem. Theory Comput., 14, 2353 (2018)

Magnetic properties of a [Dy]-complex

- Paramagnetic labeling can be useful in NMR/EPR spectroscopy to

- introduce pseudocontact shifts caused by the interaction of unpaired electrons and nuclear spins
- enable double electron-electron resonance measurements examining the coupling between two electron spins
→ distance measurement

- Example: Ln(III) complex of methyl-substituted DOTA (M8)



Häussinger *et al.*, *J. Am. Chem. Soc.*, 131, 14761 (2009)

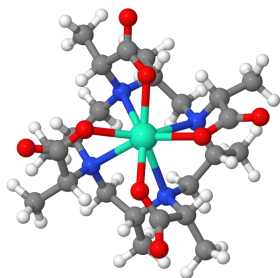
Magnetic properties of a [Dy]-complex

Required properties for paramagnetic label

- magnetic anisotropy
- spatially distributed spin-density

Our computational approach

- Four-component DMRG-CAS(n,m)CI calculations
- three orbital spaces:
CAS(9,14), CAS(27,32), CAS(27,58)



$[\text{Dy(III)}(\text{M8}_{\text{mod}})]^{-1}$
model complex

Magnetic properties of a [Dy]-complex

- Choice of active space?

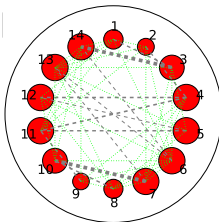
C. Stein, M. Reiher, JCTC, 2016, 12, 1760

Single-orbital entropy

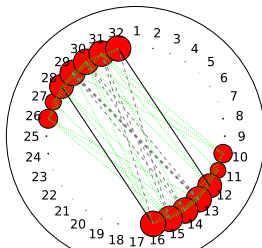
$$s_i(1) = - \sum_{\alpha=1}^4 n_{\alpha,i} \ln(n_{\alpha,i})$$

Mutual information

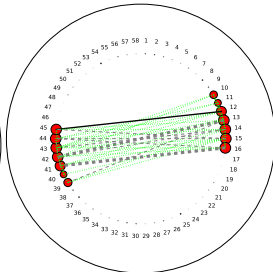
$$I_{ij} = (s_{ij}(2) - s_i(1) - s_j(1)) (1 - \delta_{ij})$$



CAS(9,14)



CAS(27,32)

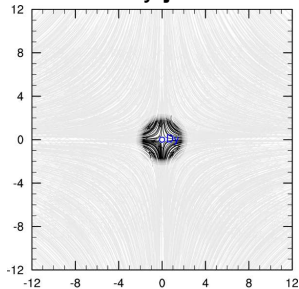


CAS(27,58)

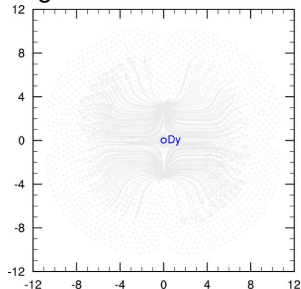
Magnetic properties of a [Dy]-complex

DMRG-CI/CAS(9,14) for a bare Dy³⁺ ion

current density $\mathbf{j} = -e\Psi^\dagger c\alpha\Psi$



magnetization $\mathbf{m} = \Psi^\dagger \Sigma \Psi$

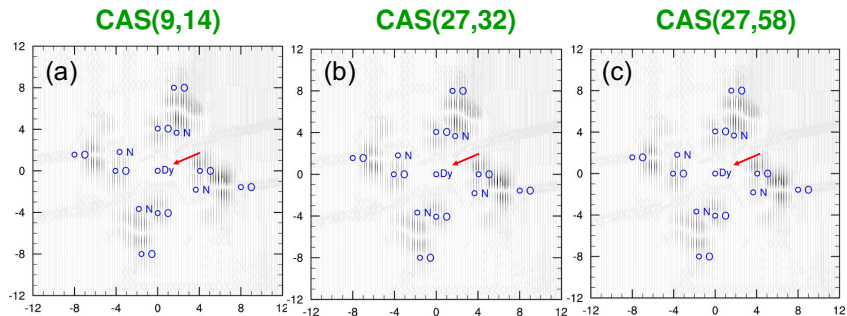


Open questions to address

- **convergence** of \mathbf{j} and \mathbf{m} wrt the active orbital space
- **magnetic anisotropy** at the [Dy] center (pseudocontact shift)?
- **spin-density** at ligand nuclei (Fermi contact shift)?

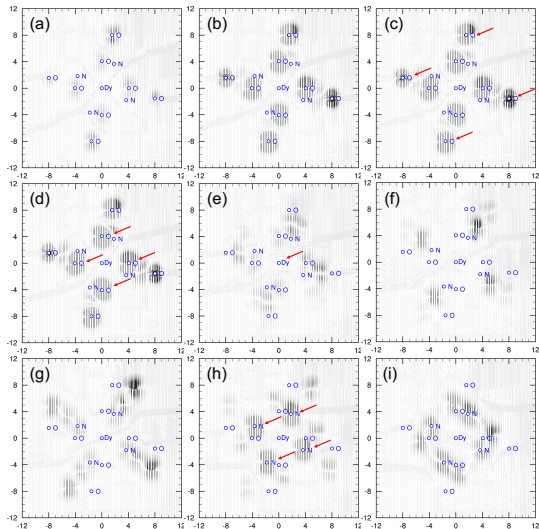
Magnetic properties of a [Dy]-complex

Current density j with ...



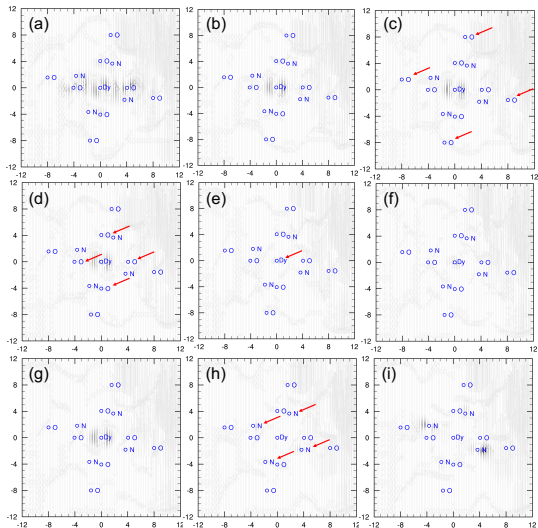
Magnetic properties of a [Dy]-complex

Current density \mathbf{j} with CAS(27,32)



Magnetic properties of a [Dy]-complex

Magnetization m with CAS(27,32)



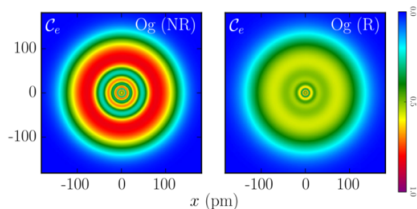
Magnetic properties of a [Dy]-complex



Battaglia, Keller, Knecht, J. Chem. Theory Comput., 14, 2353 (2018)

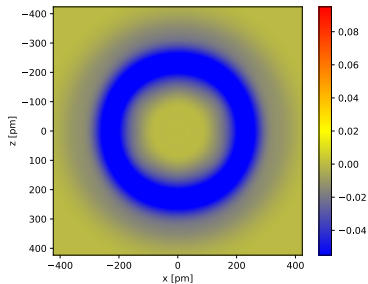
Electronic structure theory for SHEs

Electron localization function (ELF)



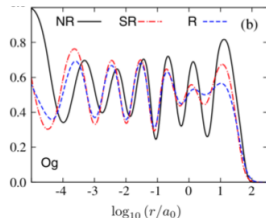
- ELF from non-relativistic and relativistic HF calculations

Jerabek *et al.*, *Phys. Rev. Lett.*, **120**, 053001 (2018)

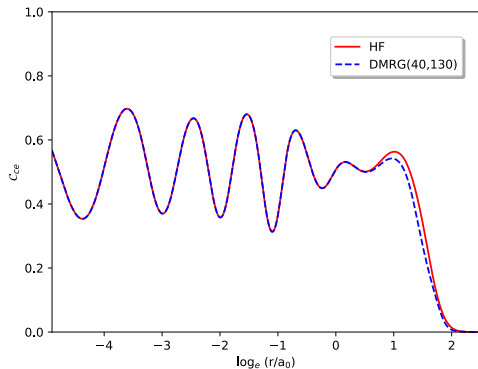


- $\Delta_{\text{ELF}}^{\text{relativistic}}$ (HF-DMRG(40,130))

Knecht, *Nachr. Chem.*, **67**, 57 (2019)

ELF as a function of the distance from the nucleus

Jerabek *et al.*, Phys. Rev. Lett., **120**, 053001 (2018)

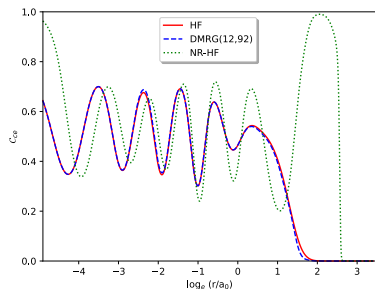


Knecht, Nachr. Chem., **67**, 57 (2019)

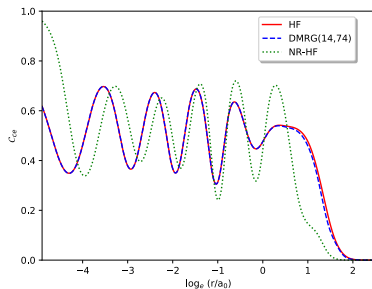
Copernicium and Flerovium

ELF as a function of the distance from the nucleus

Copernicium



Flerovium



Knecht, unpublished

Coupling to (strong) external magnetic fields



MPS for strong magnetic fields

- Atoms and molecules may exhibit exotic chemistry in strong magnetic fields
- Strong magnetic fields open up for new molecular bonding mechanism (“perpendicular paramagnetic bonding”)

Lange et al., Science, 337, 327 (2012)

- Replace momentum operator $\hat{\mathbf{p}}$ by adding a vector potential $\mathbf{A}(\mathbf{r})$

$$\hat{\boldsymbol{\pi}} = \hat{\mathbf{p}} + \mathbf{A}(\mathbf{r}) \quad \xrightarrow[\text{gauge}]{\text{Coulomb}} \quad \mathbf{A}(\mathbf{r}) = \frac{1}{2} \mathbf{B} \times (\mathbf{r} - \mathbf{r}_G)$$

- Use gauge-including atomic orbitals (GIAOs) as a basis:

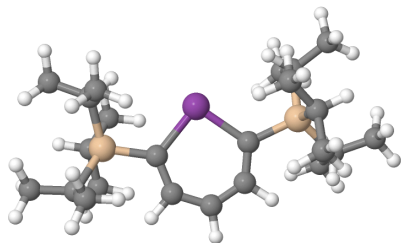
$$\phi_x^{\text{GIAO}}(\mathbf{r}) = \phi_x(\mathbf{r}) \exp(-i\mathbf{A}(\mathbf{R}) \cdot \mathbf{r}) \quad (57)$$

- Interaction with magnetic field breaks time-reversal symmetry!

Interplay of magnetic field strength and orbital entropies

Knecht, unpublished

- Exploratory relativistic 4c-DMRG-CI calculations ($m = 384$)
- Basis sets
 - Bi: *uncontracted* ANO-RCC
 - C: ANO-RCC-DZVP
 - ANO-RCC-MB otherwise
- Customized fitting basis sets

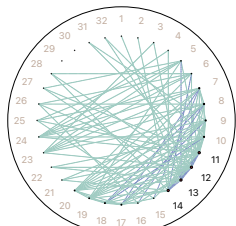


“Bismabenzene”

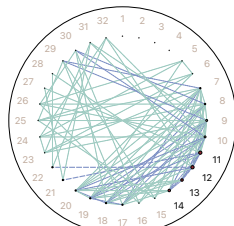
Ishii *et al.*, JACS, 138, 12787 (2016)

→ Visualize orbital entropies as a function of the magnetic field strength (z -axis)

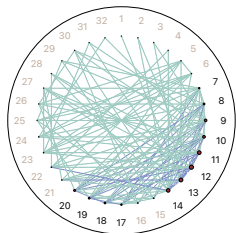
Interplay of magnetic field strength and orbital entropies



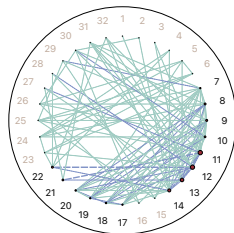
B = 0 T



B = 3 T



B = 300 T



B = 600 T

Thank you for your kind attention